FULL PAPER

Dual-Mechanism Antimicrobial Polymer–ZnO Nanoparticle and Crystal Violet-Encapsulated Silicone

*Sacha Noimark, Jonathan Weiner, Nuruzzaman Noor, Elaine Allan, Charlotte K. Williams, Milo S. P. Shaffer, and Ivan P. Parkin**

The prevalence of healthcare-associated infection caused by multidrug-resistant bacteria is of critical concern worldwide. It is reported on the development of a bactericidal surface prepared by use of a simple, upscalable, two-step dipping strategy to incorporate crystal violet and di(octyl)-phosphinic- acid-capped zinc oxide nanoparticles into medical grade silicone, as a strategy to reduce the risk of infection. The material is characterized by UV–vis absorbance spectroscopy, X-ray photoelectron spectroscopy (XPS), inductively coupled plasma-optical emission spectroscopy (ICP-OES) and transmission electron microscopy (TEM) and confirmed the incorporation of the ZnO nanoparticles in the polymer. The novel system proves to be a highly versatile bactericidal material when tested against both *Staphylococcus aureus* and *Escherichia coli*, key causative micro-organisms for hospital-acquired infection (HAI). Potent antimicrobial activity is noted under dark conditions, with a significant enhancement exhibits when the surfaces are illuminated with a standard hospital light source. This polymer has the potential to decrease the risk of HAI, by killing bacteria in contact with the surface.

1. Introduction

Despite rigid hygiene protocols in place, the transfer of bacteria within hospital environments is a substantial issue and can lead to the contraction of healthcare-associated infection. Increasingly, these outbreaks are caused by multidrug-resistant bacteria and can be extremely difficult to treat, often significantly extending the length of hospital stay and causing additional discomfort and pain to the patient. The Centers for Disease Control and Prevention (CDC) have released a publication, which details that the estimated cost of hospital-acquired infections (HAIs) to US hospitals ranges up to $ 45 billion for inpatient hospital services[1] and in 2011, ca. 75 000 hospitalized patients with HAIs died.[2] However, many of these infections are preventable and effective infection control interventions can save US healthcare institutions up to $ 31.5 billion.[1]

One strategy to minimize the spread of infection is the use of antimicrobial surfaces.[3] Many such materials have been prepared for both hard and soft surfaces, for example, the use of micro-biocide releasing surfaces,[4,5] silver-ion technology,[6,7] copper surfaces,[8–13] or surfaces covalently attached to peptides.[14–16]

One slightly different approach involves the photosensitization of bacteria. Light-activated antimicrobial hard surfaces, such as those coated with titania or doped titania thin films,[17–20] or photobactericidal polymers, embedded with photosensitizer dyes,[21–31] exhibit potent light-activated antimicrobial activity.

Visible light photoactive antimicrobial surfaces including titania, silver-loaded titania, nitrogen-doped titania, and silver-loaded nitrogen-doped titania thin films, on glass surfaces have been developed.[17,19] Under white lighting conditions (12 h irradiation), titania coatings demonstrate negligible antimicrobial activity when tested against EMRSA-16.[17] Since titania is a UV-active photocatalyst, this poor photoactivity can be attributed to the limited proportion of UV light present in the white light source[17] and therefore, these materials are not suitable for white light-activated touch surface applications. Silver-doped titania-coatings have shown an enhanced photocatalytic effect, reducing bacterial numbers by ca. 2.5 log.[17] Moreover, when tested against *E. coli,* these samples demonstrate efficacious bacterial kills, even under dark conditions, reducing bacterial numbers to below the detection limit within 6 h.[17] Similarly, silver-loaded nitrogen-doped titania samples also demonstrate enhanced light-activated kill rates compared to titania coatings, reducing bacterial levels to below the detection limit within 5 h at a light fluence of 1000 lx, although less efficacious antimicrobial activity was noted under dark conditions.[19] When tested against MRSA however, these samples only affected a 2 log reduction in bacterial numbers upon irradiation for 5 h.[19]

S. Noimark, Dr. N. Noor, Prof. I. P. Parkin
Materials Chemistry Research Centre
Department of Chemistry
University College London
20 Gordon St, London, WC1H 0AJ, UK
E-mail: i.p.parkin@ucl.ac.uk
J. Weiner, Prof. C. K. Williams, Prof. M. S. P. Shaffer
Department of Chemistry
Imperial College London
London, SW7 2AZ, UK
Dr. E. Allan
Division of Microbial Diseases
UCL Eastman Dental Institute
University College London
256 Grays Inn Road, London, WC1X 8LD, UK

The copyright line for this article was changed on 14 January 2015 after original online publication.

FULL PAPER

Light-activated antimicrobial polymeric surfaces can be prepared using a simple "swell-encapsulation-shrink" strategy to incorporate photosensitizer dye molecules into medical-grade polymers,[23–27] and this method can be upscaled for commercial production. Illumination of dye-incorporated polymers promotes the dye molecule to an excited triplet state, via intersystem crossing from the photoexcited dye singlet state.[32] The triplet state interacts with surrounding molecules such as molecular oxygen, generating reactive oxygen species that initiate a non-site specific attack against bacteria in the vicinity, causing oxidative damage and resulting in cell death.[26] Due to the multiple mechanisms of microbial attack induced by a range of photogenerated reactive oxygen species, the emergence of resistance to this antimicrobial strategy is unlikely.[33] These materials have induced the lethal photosensitization of both Gram-positive and Gram-negative bacteria,[21–24] with enhanced activity upon the additional encapsulation of 2 nm gold nanoparticles, attributed to an increased dye triplet state production.[22,25,27] Moreover, some photobactericidal surfaces also demonstrated significant kill under dark conditions, over long time periods.[34]

Whereas other bactericidal surfaces lose efficacy due to the build-up of dirt obscuring the antimicrobial properties, it is anticipated that the photogenerated species produced by these samples can oxidize organic contaminants on the polymer surface, maintaining the surface anti-infective properties. Photobactericidal polymers have also demonstrated the laser-activated reduction of *Staphylococcus epidermidis* biofilm formation,[35] a crucial property for polymers developed for use in medical devices. However, one drawback is that it has proven difficult to synthesize aqueously dispersed gold nanoparticles within the narrow size constraints required for the enhanced antimicrobial efficacy and to purchase commercially produced gold colloid is relatively expensive.

Zinc oxide is a naturally occurring metal oxide; it is inexpensive, has a high thermal conductivity and a wide band gap (3.36 eV) lending itself to a large range of commercial applications from paint pigmentation to field effect transistors, gas sensors, and in photovoltaics. Zinc oxide is generally considered to be safe and has widespread use as a food additive,[36] in food packaging,[37] and in skin ointments. In fact, it is commonly used to treat diaper rashes[38,39] and also widely used in sunscreen products as it is an effective block of UV radiation.[38,40] Recently, zinc oxide nanoparticles have attracted heightened research interest in terms of their semiconductor properties, in addition to their bactericidal activity. They exhibit antibacterial properties against a range of both Gram-positive and Gram-negative bacteria through a cytotoxic mechanism, in addition to showing activity against high-temperature and -pressure resistant spores and fungal pathogens.[41–45] It has been suggested that the mechanism by which zinc oxide nanoparticles demonstrate antimicrobial activity may involve the accumulation of nanoparticles in the outer membrane or cytoplasm of bacterial cells, or may be attributed to the generation of reactive oxygen species.[45] Reports have also indicated that zinc oxide nanoparticles may disrupt or damage bacterial cell membranes, resulting in the leakage of intracellular components, or cause oxidative stress.[46,47] Zinc oxide nanoparticles also demonstrate an enhanced antimicrobial efficacy, when compared to bulk zinc oxide.[42,44] This can be attributed to the high surface area to volume ratio of nanoparticles.[42] Moreover, it

has also been observed that there exists a size dependency on the antimicrobial activity of the zinc oxide nanoparticles, with decreasing nanoparticle size resulting in greater activity.[41,44,45]

Since nanoparticulate zinc oxide is insoluble in most solvents, in order to disperse the nanoparticles, large excesses of surfactant are often added. However, the presence of surfactant can reduce performance. To overcome these adverse effects and obviate the need for excess surfactant, a synthetic organometallic route to zinc oxide via hydrolysis of zinc alkyl groups in the presence of nonhydrolyzable zinc carboxylates can be used.[48,49] Recently, it has been noted that the use of zinc di(octyl) phosphinate surface groups enhances solubility of the nanoparticles, improving its catalytic performance in methanol synthesis.[50] The resultant small zinc oxide nanoparticles (3–4 nm) are easily dispersed in toluene and can be encapsulated into polymers using a simple swelling strategy.

In this paper, the use of a two-step dipping process to incorporate zinc oxide nanoparticles in combination with a commercially available photosensitizer dye, crystal violet, into medical-grade silicone is reported on. In addition to characterization by UV–vis absorbance spectroscopy, transmission electron microscopy (TEM) was used to analyze the nanoparticle-embedded polymer and demonstrated evidence of nanoparticle incorporation. The antimicrobial activity of the crystal violet-coated, nanozinc-oxide-encapsulated polymer was tested against both Gram-negative and Gram-positive bacteria ubiquitous in healthcare settings and a white light source comparable to standard hospital lighting conditions was used to enhance the antimicrobial properties of the novel material. Surprisingly, significant kill was achieved against both bacteria under dark conditions, with a significant enhancement in bactericidal activity demonstrated upon white light illumination.

2. Results

2.1. Material Synthesis and Characterization

Novel antimicrobial crystal violet-coated, zinc-oxide-encapsulated silicone polymers were prepared using a simple two-step dipping procedure. In the first dipping step, the silicone polymers were immersed in a ZnO nanoparticle/toluene swelling solution (1 mg mL^{-1} ZnO nanoparticles) for 24 h, for optimal zinc oxide nanoparticle incorporation throughout the polymer bulk and no change in polymer coloration was observed upon use of the "swell-encapsulation-shrink" strategy. Post-treatment with an aqueous crystal violet solution (0.001 mol dm^{-3}, 72 h) resulted in a purple colored polymer (**Figure 1**) and as has been optimized previously,[26] the uptake of the dye was a predominantly surface process at this concentration. It should be noted that the rate of surface uptake of the dye can be increased and reduced to ca. 4 h by heating the dipping solution to 40 °C.

UV–vis absorbance spectroscopy analysis of the swelling solutions used for sample preparation demonstrated a characteristic shoulder at 350 nm for the dispersed ZnO nanoparticle solution,[50] whereas the capping agent solution and Zn(DOPA)$_2$ exhibited no significant absorption in this region (**Figure 2**a). Using a Tauc plot (see Supporting Information 2.1), the band onset of the nanoparticle suspension was estimated at 3.53 eV (Figure 2a, inset), indicating that the ZnO nanoparticle
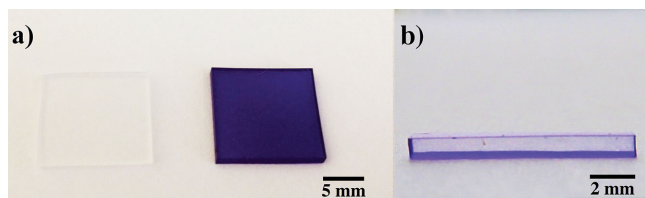
Figure 1. a) Photograph of the zinc oxide nanoparticle-encapsulated silicone sample and the crystal violet-coated, zinc oxide nanoparticle-encapsulated silicone sample. b) Cross-sectional photograph of the zinc-oxide nanoparticle encapsulated, crystal violet-coated silicone sample. The sample dimensions are 1.1 cm × 1.1 cm × 0.1 cm.

is a UV photocatalyst (<385 nm) and should not exhibit significant white light-activated antimicrobial activity. UV–vis absorbance spectroscopy was also used to examine the materials prepared for microbiological testing (Figure 2b). When encapsulated in silicone, no characteristic UV–vis signal of the ZnO nanoparticles was noted. This can be attributed to low polymer nanoparticle concentrations and significant UV–vis absorption signal of the silicone substrate in the region 250–350 nm. The UV–vis absorbance signals of both the crystal violet-coated silicone samples and the crystal violet-coated, zinc oxide-embedded silicone samples were similar in peak shape and position and characteristic of the crystal violet dye, with absorbance maxima at $\lambda \approx 590$ nm and a shoulder peak at $\lambda \approx 545$ nm. This indicates that the presence of the zinc oxide nanoparticles does not affect the position of spectral features.

X-ray photoelectron spectroscopy (XPS) analysis of the nanoparticle powder identifies a doublet in the Zn-2p region corresponding to zinc in ZnO (see Supporting Information, 2.2a). XPS of the crystal violet-coated, zinc oxide nanoparticle-encapsulated silicone polymer showed evidence of nanoparticle encapsulation (see 2.2b-e, Supporting Information). A doublet in the Zn (2p) region corresponding to zinc in ZnO was identified, confirming the presence of zinc oxide nanoparticles within the polymer. Peaks in the O (1s) region, and C (1s) region Si (2p) region, and N (1s) region were also present, correlating to the presence of the nanoparticle, polymer and crystal violet dye (N peak). Inductively coupled plasma-optical emission

spectroscopy (ICP-OES) was used to determine whether ZnO or other zinc species leached from the polymer into solution. Samples of silicone embedded with ZnO (1.1 × 1.1 × 0.1 cm) were immersed in distilled water and the concentration of zinc released into solution, was measured periodically. Results indicated that small traces of zinc leached into solution (up to 0.0025 mg of zinc per sample) over the 3 weeks experimental duration (full results in Supporting Information, 2.3).

TEM of toluene dispersed zinc oxide nanoparticle powder drop cast onto TEM grids shows well-separated, small, spherical nanoparticles with no evidence of agglomeration (**Figure 3**). Size analysis showed an average nanoparticle diameter of 3.3 nm (±1.1 nm), which is similar to that calculated from the UV–vis. HR-TEM images showed the particles to be crystal-line with lattice spacings correlating with Wurtzite ZnO. Each nanoparticle was composed of a single-crystalline domain, a result of the nucleation controlled growth and the prevention of oriented attachment by the strongly bound di(octyl)phosphinate ligand. TEM analysis of the ZnO nanoparticle-embedded polymer edge demonstrated evidence of nanoparticle encapsulation, with visible crystallographic planes present (Figure 3C). Lattice spacings of 0.28 nm were observed correlating to the (100) plane of hexagonal ZnO.

The photostability of crystal violet- and crystal violet-coated, zinc oxide nanoparticle-encapsulated silicone polymers under white hospital light source conditions, was examined using UV–vis spectroscopy (see Supporting Information, 2.4). The crystal violet-coated samples demonstrated strong photostability under ambient lighting conditions and even under the intense lighting conditions used in this study - 31 x more intense that that typical of hospital wards and corridors (ca. 200 lx).[29] The photodegradation of the crystal violet-coated silicone polymers was ca. 59% over a period of 61 d. Over the same period of time, the crystal violet-coated, zinc oxide-encapsulated polymer resulted in a 35% photodegradation of the crystal violet dye, indicating that the ZnO nanoparticles did not degrade the dye and interestingly, the presence of the nanoparticles may in fact stabilize the dye with respect to photodegradation. These stabilization effects are an area of interest for future research. These samples demonstrate suitability for use as photo-activated
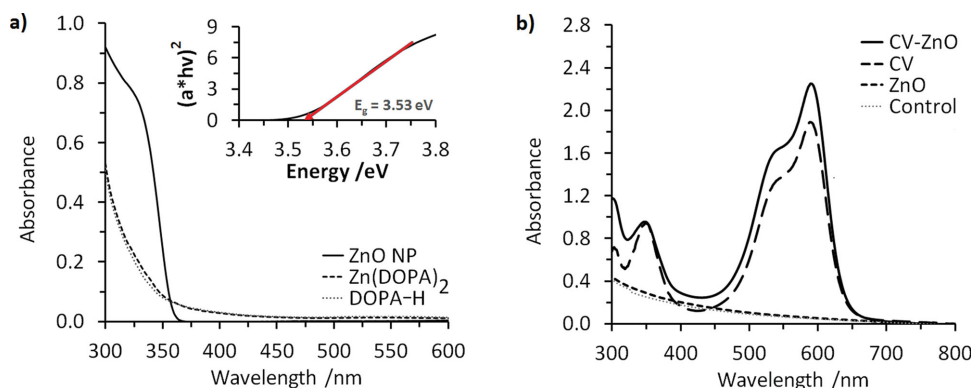
Figure 2. a) UV–vis absorbance spectra of toluene-dispersed di(octyl)phosphinic acid-capped zinc oxide nanoparticles (ZnO NP), di(octyl)phosphinic acid in toluene (DOPA-H) and zinc bis(di(octyl) phosphinate) (Zn(DOPA)$_2$) in toluene. Inset: Tauc plot to determine bandgap of di(octyl)phosphinic acid-capped zinc oxide nanoparticles. The band onset of the 3–4 nm zinc oxide nanoparticles was calculated as 3.53 eV. b) UV–vis absorbance spectra of modified samples used for microbiological testing: Solvent-treated silicone (control), crystal violet-coated-silicone (CV), zinc oxide nanoparticle-encapsulated-silicone (ZnO) and crystal violet-coated, zinc oxide nanoparticle-encapsulated silicone (CV-ZnO).
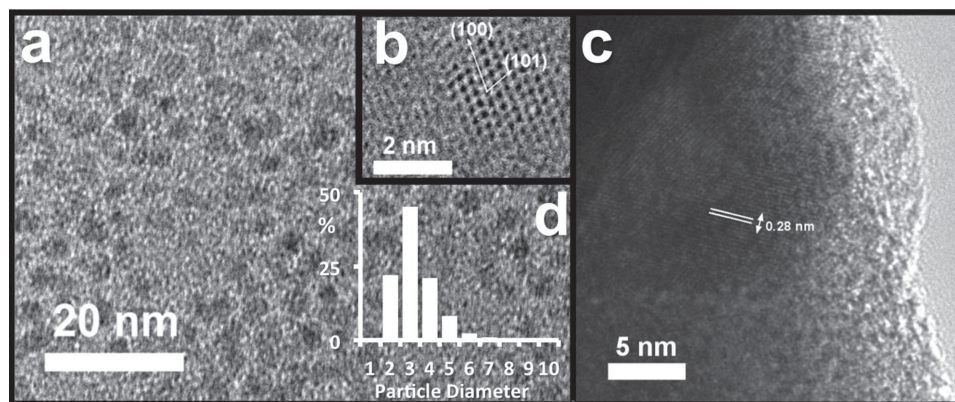
Figure 3. a) TEM of zinc oxide nanoparticles with di(octyl) phosphinate capping ligands, b) HR-TEM of zinc oxide nanoparticle with lattice spacings and c) silicone polymer encapsulated with zinc oxide nanoparticles with di(octyl) phosphinate capping ligands. d) Histogram of particle size distribution of zinc oxide nanoparticles as synthesized, determined by TEM.

antimicrobial surfaces under the laboratory testing conditions investigated indicating that under ambient lighting in idealized conditions, these samples would demonstrate long-term photostability. It should be noted that in healthcare applications where the surfaces are constantly exposed to harsh chemical cleaning treatments and there is frequent surface contact, the material stability may be reduced, however, it is anticipated that these surfaces should maintain potency for several years.

2.2. Microbiological Testing

The antimicrobial activity of a series of modified medical-grade silicone samples was determined using representative Gram-positive and Gram-negative bacteria, *S. aureus* and *E. coli*, respectively, both of which are commonly found in healthcare environments. For each experiment, a set of samples were illuminated with a 28 W white hospital light source, emitting an average light intensity of 3750 lux at a distance of 30 cm, while a parallel set was stored under dark conditions for the same duration. Although the white light intensity used in this investigation is approximately three times that found in a typical A & E examination room,[29] the microbial loads used in these experiments far surpass those typically found in a clinical environment, to test the potency of these antimicrobial surfaces ($\approx$45 529 cfu cm^{-2} used in this investigation, compared to $\leq$3060 cfu cm^{-2} with average values of <100 cfu cm^{-2} in a clinical environment[12,13,34,51,52]).

The photo-activated and intrinsic bactericidal activities of the following samples were tested: solvent-treated silicone, a crystal violet-coated silicone (CV), a di(octyl)phosphinic acid-capped zinc oxide nanoparticle-encapsulated silicone (ZnO), a di(octyl)-phosphinic acid-encapsulated silicone (DOPA-H), a zinc bis(di(octyl) phosphinate-encapsulated silicone (Zn(DOPA)$_2$), and a crystal violet-coated, di(octyl) phosphinic acid-capped zinc oxide nanoparticle encapsulated silicone (CVZnO). This range of samples was tested to deduce whether it was the ZnO nanoparticle, free capping agent or the ZnO-bound capping agent, that contributed to the antimicrobial activity. Samples were also coated with crystal violet dye to establish whether this enhances bacterial kills and if there exists a

similar synergistic enhancement in the antimicrobial activity as previously established with crystal violet, methylene blue and gold nanoparticle combinations encapsulated into medical-grade polymers.[22,26,27,34]

Under dark conditions (1 h incubation), neither the ZnO sample nor the DOPA-H sample demonstrated significant activity when tested against *S. aureus*, although the Zn(DOPA)$_2$ sample induced a statistically significant reduction in staphylococcal numbers ($P < 0.001$) (**Figure 4**a). The CVZnO sample significantly reduced the number of viable *S. aureus* on the sample surface ($P < 0.001$), with enhanced bacterial kills compared to the CV sample. This can be attributed to the higher concentration of crystal violet at these sample surfaces due to the preswelling treatment in toluene, used to encapsulated the ZnO nanoparticles. Illumination of these samples using a standard hospital lighting source for just 1 h resulted in the lethal photosensitization of *S. aureus* on the CV sample (1.69 log kill), with a marked increase in antimicrobial activity on the CVZnO sample ($P < 0.001$, 3.36 log kill).

A correlation has been noted in the literature between the decreasing size of the zinc oxide nanoparticle and its bactericidal efficacy.[41,44,45] In this study, small 3–4 nm ZnO nanoparticles were incorporated into the polymer. These polymers exhibited antimicrobial activity against *E. coli*, with a statistically significant reduction in bacterial numbers (1.41 log) following incubation for 6 h in the dark ($P < 0.001$, Figure 4). ICP-OES studies indicated that small traces of zinc species leached from the polymer when left in aqueous solution for extended periods. However, previous research has shown that leached Zn^{2+} ions are unlikely to contribute to the antimicrobial activity.[45]

Illumination of the ZnO sample resulted in enhanced antimicrobial activity with a 1.9 log reduction in bacterial numbers for the same incubation duration. No antimicrobial activity was observed on the DOPA-H and Zn(DOPA)$_2$ samples either under dark conditions or with white light illumination for 3 h and therefore, these samples were not tested for an extended duration of 6 h. CV samples demonstrated a limited, but statistically significant bactericidal activity when tested against *E. coli* (0.72 log kill, 6 h illumination). This discrepancy between the efficacy of photodynamic therapy (PDT) against Gram-positive bacteria and Gram-negative bacteria can be attributed to

www.MaterialsViews.com

ADVANCED
FUNCTIONAL
MATERIALS
www.afm-journal.de

FULL PAPER
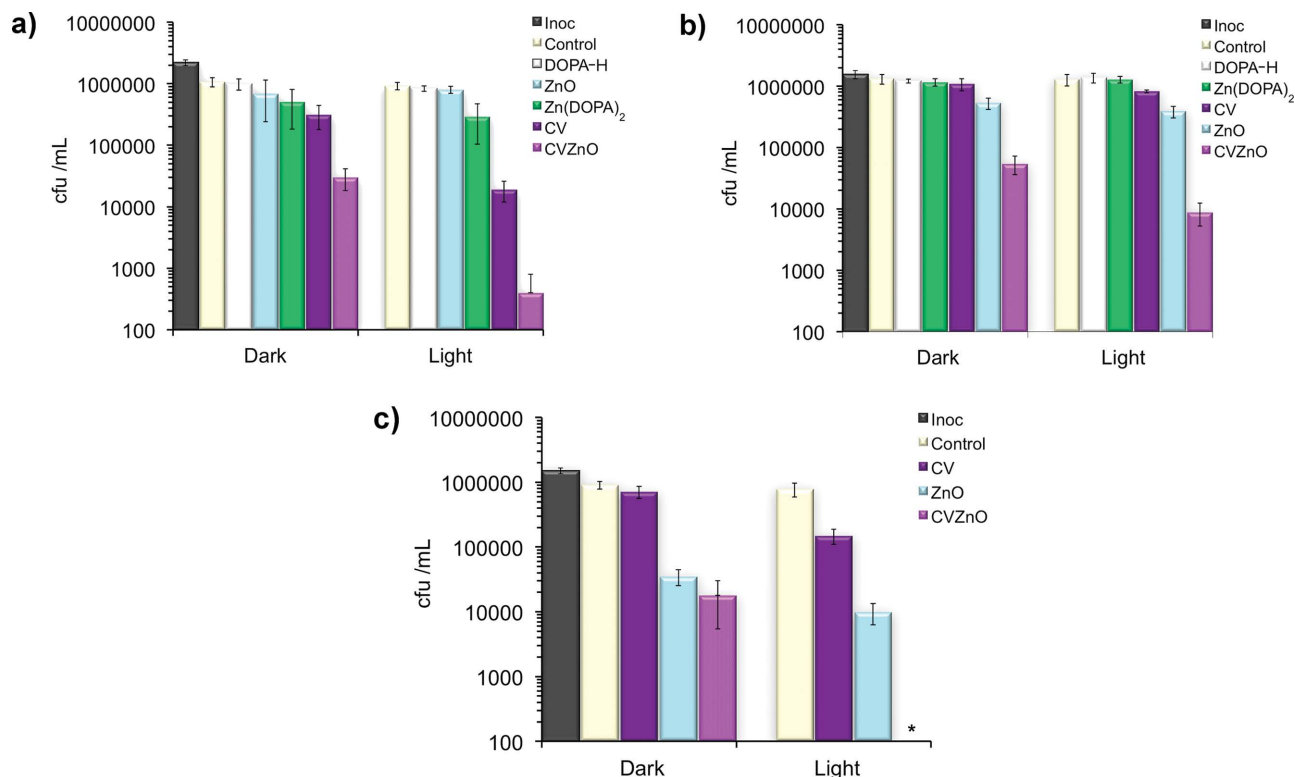
Figure 4. Graph to show the viable counts of bacteria after incubation on modified silicone polymers exposed to white light illumination: a) *S. aureus* (1 h illumination), b) *E. coli* (3 h illumination), and c) *E. coli* (6 h illumination). The white light hospital lighting source emitted an average light intensity of 3750 ± 250 lux at a distance of 30 cm from the samples indicates where the bacterial counts were reduced to below the detection limit of 100 cfu.

differences in their cell wall structures.[26] Gram-negative bacteria have both an inner and outer cell membrane composed of phospholipid bilayers embedded with lipopolysaccharides and proteins, whereas Gram-positive bacteria have a single-inner phospholipid bilayer cellular membrane surrounded by peptidoglycan and this acts as an ineffective barrier against PDT. It has also been noted that the inherent bactericidal efficacy of crystal violet against Gram-negative bacteria is more limited.[26] However, the dual-combination CVZnO sample exhibited potent photobactericidal activity against *E. coli*, with bacterial numbers reduced by 2.16 log within 3 h white light illumination and to below the detection limit in 6 hours (*P* < 0.001). This suggests a synergistic effect in the activity of the triarylmethane dye when ZnO nanoparticles are present, as enhancements in bacterial kills were noted, that surpassed kills demonstrated if they were caused by an additive effect.

Overall, the results indicate that the ZnO samples demonstrate a stronger bactericidal activity against the Gram-negative bacterium, *E. coli*, than the Gram-positive, *S. aureus*. Conversely, the CV samples induce the lethal photosensitization of *S. aureus*. Crystal violet is known to exhibit antimicrobial activity against Gram-positive bacteria and is used in the treatment of superficial wounds and some skin infections.[53–57] Consequently, this novel ZnO-dye combination creates an antimicrobial surface on medical-grade silicone, effective against both *E. coli* and *S. aureus*. The CVZnO sample demonstrates superior antimicrobial activity, inducing the lethal photosensitization of both *S. aureus* and *E. coli*, with high reductions in

viable bacterial numbers achieved after only 1 h and 6 h illumination, respectively. Moreover, significant kills were also observed under dark conditions and importantly, a highly significant reduction in *E. coli* numbers (1.70 log) was recorded with CVZnO after 6 h incubation. These samples achieved a 1.16 log greater reduction in bacterial numbers when tested against *E. coli* under dark conditions (6 h), compared to our previously synthesized most effective samples, which were incorporated with methylene blue, crystal violet, and 2 nm gold nanoparticles.[34] It is clear that the zinc oxide nanoparticle, dye-coated silicone samples exhibit stronger antimicrobial activity than other dye-nanoparticle samples investigated under dark conditions, while their activity is comparable to that demonstrated by a previously tested multi-dye-nanogold-encapsulated silicone[34] under illumination.

To validate the antimicrobial effectiveness of these surfaces, their photobactericidal activity was compared to other antimicrobial systems published in the literature. Limited data have been published on the development of photobactericidal polymers. One system details the synthesis of protoporphyrin- and zinc protoporphyrin-grafted nylon fibers using a white light source of intensities ranging from 10 000 to 60 000 lux, to activate the antimicrobial properties.[28] When tested against *S. aureus* these samples induced the lethal photosensitization of bacteria within 30 min, reducing bacterial numbers to 5.6% on the zinc protoporphyrin sample at a light fluence of 40 000 lx;[28] however, no antimicrobial activity was observed when tested against *E. coli* at this light fluence.[28] These results

FULL PAPER

highlight the potent light-activated antimicrobial activity demonstrated by the CVZnO surfaces reported here, achieving the lethal photosensitization of both *S. aureus* and *E. coli*.

These antimicrobial polymers can also be compared to other antimicrobial surfaces, including visible light photoactive antimicrobial titania, silver-loaded titania, nitrogen-doped titania, and silver-loaded nitrogen-doped titania thin films on glass surfaces.[17,19] Some of these antimicrobial systems demonstrate poor antimicrobial efficacy compared with the CVZnO silicone reported here.[17,28] However, other systems exhibited comparable, or enhanced antimicrobial activity.[11,19] The use of thin-film antimicrobial coatings, or copper surfaces however, presents a substantial financial burden to healthcare institutions. Existing furnishings would have to be replaced with the antimicrobial equivalent and UK hospitals that are part of the Private Finance Initiative scheme would also be required to pay an upfront "30 year lifetime cost" for new furnishing installations. The use of an antimicrobial polymer that can be retrofit onto existing furnishings presents a promising, inexpensive alternative for use as an infection-control mechanism.

It is anticipated that this crystal violet-zinc oxide-polymer technology can be utilized to develop antimicrobial surfaces for use, chiefly in healthcare environments, but also in everyday applications such as keyboards, mobile phone, and tablet covers and kitchen surfaces. Although this novel material has been developed for use in touch surfaces rather than implanted medical devices, it is crucial that these surfaces are nontoxic and contact with them do not affect adverse reactions. With the widespread use of ZnO nanoparticles in the cosmetics and food industry, their toxicity has been extensively studied in a number of reports. The toxicity of nanoparticles to humans depends on a number of factors including their size, shape, route of administration, and dosage.[58] These nanoparticles demonstrate low toxicity to mammalian cells, with investigations concluding that ZnO nanoparticle penetration through the skin is negligible and through other routes of administration ZnO only showed toxic effects at high doses (>100 μg mL^{-1}).[59–61] Crystal violet also poses a low toxicity risk and was used as a topical antiseptic before its use was superseded by modern drugs.[62] The World Health Organization also recommended its inclusion in the "Interagency Emergency Health Kit"[63] and clinical trials have investigated its efficacy as a potential treatment against MRSA.[64,65] However, it should be noted that the release of nanoparticles such as copper oxide, zinc oxide, and silver, from household products into waste streams can pose a threat to "non-target" aquatic organisms.[66] In this application, the nanoparticles are embedded within a polymer, with low leaching concentrations documented and it is anticipated that these antimicrobial surfaces would be used in "dry" applications and therefore should not pose an additional risk to aquatic organisms. Consequently, the use of this antimicrobial combination in these novel dual-mechanism antimicrobial surfaces should not present a risk to users and should maintain low surface bacterial levels, reducing the likelihood of the spread of infections in a hospital environment.

3. Conclusion

Highly efficacious antimicrobial surfaces have been synthesized using a straightforward and simple two-stage dipping process.

Incorporation of both ZnO nanoparticles and crystal violet dye into medical-grade silicone resulted in one of the most effective antimicrobial polymer surfaces that has been developed to date. This material demonstrates bactericidal activity via a novel dual-mechanism approach, utilizing PDT in combination with the inherent antimicrobial properties of zinc oxide nanoparticles, such that the resultant polymer exhibits potent bactericidal behavior, with significant bacterial kills achieved within 1 h against Gram-positive bacteria and within 6 h against Gram-negative bacteria in both dark and illuminated conditions.

These antimicrobial materials present ideal surfaces for use in healthcare environments. Moreover, it can be speculated that due to the multiple bacterial attack mechanisms present associated with the component antimicrobial agents, bacterial resistance to this novel multiple-mechanism antimicrobial surface is unlikely.

Supporting Information

Supporting Information is available from the Wiley Online Library or from the author.

[1] R. D. Scott II, The direct medical costs of healthcare-associated infections in U.S. hospitals and the benefits of prevention, March 2009.

[2] Healthcare-associated infections, http://www.cdc.gov/HAI/surveillance/index.html, (accessed: August 2014).

[3] S. Noimark, C. W. Dunnill, I. P. Parkin, *Adv. Drug Delivery Rev.* **2013**, *65*, 570.

[4] C. E. Edmiston, F. C. Daoud, D. Leaper, *Surgery* **2013**, *154*, 89.

[5] D. L. Williams, K. D. Sinclair, S. Jeyapalina, R. D. Bloebaum, *J. Biomed. Mater. Res. Part B: Appl. Biomater.* **2013**, *101B*, 1078.

[6] Acrymed Inc., SilvaGard technology summary, http://www.acrymed.com/pdf/SilvaGard%20Technical%20Summary.pdf (accessed: July 2013).

[7] Agion silver antimicrobial, http://www.agion-tech.com, accessed on 22-07-2013.

[8] F. Marais, S. Mehtar, L. Chalkley, *J. Hosp. Infect.* **2010**, *74*, 80.

[9] A. Mikolay, S. Huggett, L. Tikana, G. Grass, J. Braun, D. H. Nies, *Appl. Microbiol. Biotechnol.* **2010**, *87*, 1875.

[10] C. D. Salgado, K. A. Sepkowitz, J. F. John, J. R. Cantey, H. H. Attaway, K. D. Freeman, P. A. Sharpe, H. T. Michels, M. G. Schmidt, *Infect. Control Hosp. Epidemiol.* **2013**, *34*, 479.

[11] I. A. Hassan, I. P. Parkin, S. P. Nair, C. J. Carmalt, *J. Mater. Chem. B* **2014**, *2*, 2855.

[12] M. G. Schmidt, H. H. Attaway, P. A. Sharpe, J. John, Joseph, K. A. Sepkowitz, A. Morgan, S. E. Fairey, S. Singh, L. L. Steed, J. R. Cantey, K. D. Freeman, H. T. Michels, C. D. Salgado, *J Clin. Microbiol.* **2012**, *50*, 2217.

www.MaterialsViews.com

ADVANCED
FUNCTIONAL
MATERIALS
www.afm-journal.de

FULL PAPER

[13] M. G. Schmidt, I. Attaway, H. Hubert, S. E. Fairey, L. L. Steed, H. T. Michels, C. D. Salgado, *Infect. Control Hosp. Epidemiol.* **2013**, *34*, 530.

[14] K. Hilpert, M. Elliott, H. Jenssen, J. Kindrachuk, C. D. Fjell, J. Körner, D. F. H. Winkler, L. L. Weaver, P. Henklein, A. S. Ulrich, S. H. Y. Chiang, S. W. Farmer, N. Pante, R. Volkmer, R. E. W. Hancock, *Chem. Biol.* **2009**, *16*, 58.

[15] K. Rapsch, F. F. Bier, M. Tadros, M. von Nickisch-Rosenegk, *Bioconjug. Chem.* **2014**, *25*, 308.

[16] F. Costa, I. F. Carvalho, R. C. Montelaro, P. Gomes, M. C. L. Martins, *Acta Biomater.* **2011**, *7*, 1431.

[17] C. W. Dunnill, K. Page, Z. A. Aiken, S. Noimark, G. Hyett, A. Kafizas, J. Pratten, M. Wilson, I. P. Parkin, *J. Photochem. Photobiol. A Chem.* **2011**, *220*, 113.

[18] Z. A. Aiken, G. Hyett, C. W. Dunnill, M. Wilson, J. Pratten, I. P. Parkin, *Chem. Vap. Deposition* **2010**, *16*, 19.

[19] C. W. Dunnill, Z. Ansari, A. Kafizas, S. Perni, D. J. Morgan, M. Wilson, I. P. Parkin, *J. Mater. Chem.* **2011**, *21*, 11854.

[20] C. W. Dunnill, Z. A. Aiken, J. Pratten, M. Wilson, I. P. Parkin, *Chem. Vap. Deposition* **2010**, *16*, 50.

[21] A. J. T. Naik, S. Ismail, C. Kay, M. Wilson, I. P. Parkin, *Mater. Chem. Phys.* **2011**, *129*, 446.

[22] S. Perni, C. Piccirillo, A. Kafizas, M. Uppal, J. Pratten, M. Wilson, I. P. Parkin, *J. Cluster Sci.* **2010**, *21*, 427.

[23] S. Perni, P. Prokopovich, C. Piccirillo, J. Pratten, I. P. Parkin, M. Wilson, *J. Mater. Chem.* **2009**, *19*, 2715.

[24] S. Perni, J. Pratten, M. Wilson, C. Piccirillo, I. P. Parkin, P. Prokopovich, *J. Biomater. Appl.* **2011**, *25*, 387.

[25] S. Noimark, C. W. Dunnill, C. W. M. Kay, S. Perni, P. Prokopovich, S. Ismail, M. Wilson, I. P. Parkin, *J. Mater. Chem.* **2012**, *22*, 15388.

[26] S. Noimark, M. Bovis, A. J. MacRobert, A. Correia, E. Allan, M. Wilson, I. P. Parkin, *RSC Adv.* **2013**, *3*, 18383.

[27] S. Perni, C. Piccirillo, J. Pratten, P. Prokopovich, W. Chrzanowski, I. P. Parkin, M. Wilson, *Biomaterials* **2009**, *30*, 89.

[28] J. Bozja, J. Sherrill, S. Michielsen, I. Stojiljkovic, *J. Polym. Sci., A: Polym. Chem.* **2003**, *41*, 2297.

[29] V. Decraene, J. Pratten, M. Wilson, *Appl. Environ. Microbiol.* **2006**, *72*, 4436.

[30] V. Decraene, J. Pratten, M. Wilson, *Curr. Microbiol.* **2008**, *57*, 269.

[31] M. Wainwright, M. N. Byrne, M. A. Gattrell, *J. Photochem. Photobiol. B Biol.* **2006**, *84*, 227.

[32] I. J. MacDonald, T. J. Dougherty, *J. Porph. Phthal.* **2001**, *5*, 105.

[33] M. R. Hamblin, T. Hasan, *Photochem. Photobiol. Sci.* **2004**, *3*, 436.

[34] S. Noimark, E. Allan, I. P. Parkin, *Chem. Sci.* **2014**, *5*, 2216.

[35] S. Perni, P. Prokopovich, I. P. Parkin, M. Wilson, J. Pratten, *J. Mater. Chem.* **2010**, *20*, 8668.

[36] M. J. Salgueiro, M. Zubillaga, A. Lysionek, R. Caro, R. Weill, J. Boccio, *Nutr. Rev.* **2002**, *60*, 52.

[37] M. Cushen, J. Kerry, M. Morris, M. Cruz-Romero, E. Cummins, *Trends Food Sci. Technol.* **2012**, *24*, 30.

[38] J. Pasquet, Y. Chevalier, E. Couval, D. Bouvier, G. Noizet, C. Morlière, M.-A. Bolzinger, *Int. J. Pharm.* **2014**, *460*, 92.

[39] A. Arad, D. Mimouni, A. Zeharia, M. Mimouni, *Dermatology* **1999**, *199*, 319.

[40] S. R. Pinnell, D. Fairhurst, R. Gillies, M. A. Mitchnick, N. Kollias, *Dermatol. Surg.* **2000**, *26*, 309.

[41] L. L. Zhang, Y. H. Jiang, Y. L. Ding, M. Povey, D. York, *J. Nanopart. Res.* **2007**, *9*, 479.

[42] P. Nagarajan, V. Rajagopalan, *Sci. Technol. Adv. Mater.* **2008**, *9*, 035004.

[43] E. Hoseinzadeh, M.-Y. Alikhani, M.-R. Samarghandi, M. Shirzad-Siboni, *Desalin. Water Treat.* **2014**, *52*, 4969.

[44] A. A. Tayel, W. F. El-Tras, S. Moussa, A. F. El-Baz, H. Mahrous, M. F. Salem, L. Brimer, *J. Food Saf.* **2011**, *31*, 211.

[45] K. R. Raghupathi, R. T. Koodali, A. C. Manna, *Langmuir* **2011**, *27*, 4020.

[46] Y. Liu, L. He, A. Mustapha, H. Li, Z. Q. Hu, M. Lin, *J. Appl. Microbiol.* **2009**, *107*, 1193.

[47] Y. Xie, Y. He, P. L. Irwin, T. Jin, X. Shi, *Appl. Environ. Microbiol.* **2011**, *77*, 2325.

[48] M. Shaffer, C. Williams, K. Orchard, N. Jones, J. Weiner, Process for producing nanoparticles, patent App. No. *WO2013164650 A2*.

[49] K. L. Orchard, M. S. P. Shaffer, C. K. Williams, *Chem. Mater.* **2012**, *24*, 2443.

[50] N. J. Brown, J. Weiner, K. Hellgardt, M. S. P. Shaffer, C. K. Williams, *Chem. Commun.* **2013**, *49*, 11074.

[51] F. Marais, S. Mehtar, L. Chalkley, *J. Hosp. Infect.* **2010**, *74*, 80.

[52] G. Hedin, J. Rynback, B. Lore, *J. Hosp. Infect.* **2010**, *75*, 112.

[53] J. W. Churchman, *J. Experimental Med.* **1912**, *16*, 221.

[54] J. Stilling, *Lancet* **1890**, *136*, 965.

[55] J. Stilling, *Lancet* **1891**, *137*, 872.

[56] M. Saji, S. Taguchi, K. Uchiyama, E. Osono, N. Hayama, H. Ohkuni, *J. Hosp. Infect.* **1995**, *31*, 225.

[57] K. Kawamoto, N. Senda, K. Shimada, K. Ito, Y. Hirano, S. Murai, *Lasers Med. Sci.* **2000**, *15*, 257.

[58] A. Nel, T. Xia, L. Madler, N. Li, *Science* **2006**, *311*, 622.

[59] T.-K. Hong, N. Tripathy, H.-J. Son, K.-T. Ha, H.-S. Jeong, Y.-B. Hahn, *J. Mater. Chem. B* **2013**, *1*, 2985.

[60] R. J. Vandebriel, W. H. De Jong, *Nanotechnol. Sci. Appl.* **2012**, *5*, 61.

[61] K. M. Reddy, K. Feris, J. Bell, D. G. Wingett, C. Hanley, A. Punnoose, *Appl. Phys. Lett.* **2007**, *90*, 213902.

[62] Chicago: American Medical Association. New and nonofficial remedies, 1939. Containing descriptions of the articles which stand accepted by the council on pharmacy and chemistry of the American Medical Association on January 1, 1939.

[63] World Health Organization, the interagency emergency health kit 2006.

[64] M. Saji, S. Taguchi, K. Uchiyama, E. Osono, N. Hayama, H. Ohkuni, *J. Hosp. Infect.* **1995**, *31*, 225.

[65] K. Kawamoto, N. Senda, K. Shimada, K. Ito, Y. Hirano, S. Murai, *Laser. Med. Sci.* **2000**, *15*, 257.

[66] O. Bondarenko, K. Juganson, A. Ivask, K. Kasemets, M. Mortimer, A. Kahru, *Arch. Toxicol.* **2013**, *87*, 1181.